LEUPHANA
UNIVERSITÄT LÜNEBURG

Two-pass friction stir welding of cladded API X65

de Lima Lessa, Cleber Rodrigo; Landell, Renan Mensch; Bergmann, Luciano; dos Santos, Jorge Fernandez; Kwietniewski, Carlos Eduardo Fortis; Reguly, Afonso; Klusemann, Benjamin

23rd International Conference on Material Forming (ESAFORM 2020)

Two-Pass Friction Stir Welding of Cladded API X65

Cleber Rodrigo de Lima Lessa[a,b,c,]*, Renan Mensch Landell[a,b], Luciano Bergmann[a], Jorge Fernandez dos Santos[a], Carlos Eduardo Fortis Kwietniewski[b], Afonso Reguly[b] and Benjamin Klusemann[a,d]

[a]*Helmholtz-Zentrum Geesthacht, Institute of Materials Research, Materials Mechanics, Solid State Joining Processes (WMP), Max-Planck-Straße 1, Geesthacht 21502, Germany*
[b]*Physical Metallurgy Laboratory (LAMEF) - PPGE3M/UFRGS, Av. Osvaldo Aranha 99 s.610, Porto Alegre 90035-190, Brazil*
[c]*Federal Institute of Rio Grande do Sul (IFRS), R. Avelino Antônio de Souza 1730, Caxias do Sul 95043-700, Brazil*
[d]*Leuphana University of Lüneburg, Institute of Product and Process Innovation, Universitätsallee 1, Lüneburg 21335, Germany*

* Corresponding author. Tel.: +49-1590-6317829; fax: +49-4152-872033. *E-mail address:* cleber.lima@hzg.de

Abstract

Cladded materials are used by the oil and gas industry due to the combination of good mechanical properties and low cost of high-strength low-alloy steel (HSLA) API 5L X65 with the excellent corrosion resistance of the Inconel 625. This combination of materials are specially used on rigid risers, where aggressive substances such as organic acids, carbon dioxide and H_2S are present inside the pipeline. Conventional arc welding processes bring typically several issues, such as long welding times, melting of the involved materials, Fe dilution inside the weld metal (generally Inconel 625) and brittle phase precipitation. Friction Stir Welding (FSW) joints can produce better mechanical properties and lower tensile residual stresses when compared with conventional arc welding processes, having at the same time greater reproducibility and control of process parameters. Thus, a two-pass FSW process on 7mm cladded API 5L X65 HSLA steel plates were analyzed, the first pass of the process consisted in welding a 4mm API 5L X65 steel layer while the second pass consists of joining the 3mm Inconel 625 layer. Detailed hardness and microstructural analysis were performed. Correlation with the underlying physical mechanisms are discussed.

1. Introduction

Joining of dissimilar materials such as Ni-based superalloys and high-strength low-alloy steels is of large interest for coating applications, such as pressure vessels and oil exploration. Nickel alloys possess numerous specific physical properties, such as low thermal expansion, high electrical resistivity and unique magnetic properties. However, the wide range and high concentration of alloying elements used make the prediction of microstructure and properties of these alloys during processing very difficult, especially when the alloys are subjected to high temperatures [1]. The alloy (Inconel© 625) is a nickel superalloy, primarily strengthened by solid solutions of

chromium, molybdenum and niobium elements as well as by the formation of secondary phases and carbides [1, 2]. Inconel 625 is normally used as a corrosion resistant alloy (CRA) coating in the oil and gas industry, where different cladding processes can be used to protect the interior of carbon steel pipes and pressure vessels. The need of the CRA is related to the high aggressiveness of the crude oil, where the presence of organic acids, hydrogen sulphide, sand, carbon dioxide and active chloride limit the use of low alloyed materials [1–4]. To obtain a better coating with high corrosion resistance it is important to use two or more layers of CRA because it reduces the amount of diluted Fe from the steel substrate into the

Inconel 625 deposition and improves the corrosion resistance properties [5].

The API 5L X65 steel is a well know pipe material that combines good weldability because of the low carbon content with high mechanical resistance due to the refined microstructure. According to the American Petroleum Institute standard, this material has a minimum yield strength of 65000 psi (448 MPa) [6].

In many commercial applications, welding is inevitable to join different components. However, fusion welding processes often result in some problems like segregation of alloying elements and precipitation effects [7]. Petrzak et al. [8] observed in Inconel 625 during the solidification process pronounced differences in chemical composition between dendrite cores and interdendritic spaces. In this case, the interdendritic spaces were enriched with Nb and Mo. The chromium and nickel segregations within dendrites in an austenitic weld metal were investigated by Cieslak et al [9]. They found that solidification produces chromium and nickel-depleted zones at the crystal core, which exhibited low corrosion resistance. The study revealed that during the solidification of the weld metal, the segregation of elements such as Cr, Mo and Nb into the grain boundaries promotes the formation of carbides and topologically closed-packed (TCP) phases like Laves, P-phase, μ-phase and σ-phase [9]. The presence of this phases reduces the corrosion resistance of the dendritic core because of the depletion of these elements [10–12]. The reduction of the corrosion resistance due to segregation is well documented for the Laves phase. The presence of the Laves phase reduces the concentration of important alloying elements (Nb, Mo, Si and Ti) in the surrounding matrix which leads to a decrease of the corrosion resistance. Therefore, to control the detrimental effects of the Laves phase, their size and distribution in the matrix must be reduced by the application of post weld heat treatments, altering the welding heat input and forcing a faster weld cooling rate [8, 13, 14]. In summary, depending on the distribution and the size of the precipitates, the mechanical properties of the weld are most likely affected as well [10, 12, 15].

Friction Stir Welding (FSW) is an attractive technology to join high-strength materials such as Nickel alloys in the oil industry or subsea engineering retaining the base metal properties or even improving them [3]. As a result of active control of the welding temperature and/or cooling rate, FSW has the capability to produce joints with excellent toughness and strength. Unfavorable phase transformations that usually occur during traditional fusion-based welding techniques can be avoided and favorable phase fractions in advanced steels can be maintained in the weld zone, thus avoiding the typical property degradations associated with fusion-based welding [16]. In recent years, FSW has been applied to Nickel based alloys where the resulting effect on mechanical properties [17] and microstructure [18, 19] is well documented but also the aspect of tool degradation [20] has been reported. Nevertheless, to best of the authors knowledge, there is no publication about FSW on API 5L X65 cladded with Inconel 625.

The scope of this study is to characterize the FSW produced joints of API 5L X65 steel plate cladded with the Nickel alloy Inconel 625. In particular, the macro and microstructure formed during FSW is studied next to the resulting microhardness. The results show that the process is feasible to meet the growing demand of the oil industry and subsea engineering.

2. Materials and Experimental Methods

2.1. Construction of base material

API 5L X65 steel plates with 500 mm side length and 19.05mm thickness represent the base material in this study. The cladded plates were manufacture in API 5L X65 steel plates. The gas tungsten arc welding (GTAW) process and AWS ER NiCrMo-3 filler metal was used to produce the Inconel 625 coating with two layers deposited. Post weld heat treatment to relieve the plate stress were performed at 630°C for 1 hour before machining. The resulting thickness of the welded plate was 7 mm, being 3 mm out of Inconel 625 CRA and 4 mm out of API 5L X65 steel. The chemical composition of the clad layer (Inconel 625) and the steel substrate (API 5L X65) are shown in Table 1.

Table 1. Chemical composition (wt. %) of the API 5L X65 substrate and the Inconel 625 used to produce the clad layer.

Alloy	Ni	C	Cr	Mn	Mo	Nb	Fe
Inconel 625	65.1	0.006	21.81	-	8.63	3.48	0.44
API 5L X65	-	0.069	0.02	1.43	-	0.04	98.01

Alloy	Cu	Ti	Si	Ta	P	S	Al
Inconel 625	0.2	0.17	0.04	0.05	0.007	-	0.15
API 5L X65	-	0.015	0.32	-	0.14	0.001	0.042

2.2. Welding process procedure

The procedure used was a butt joint with two welding passes. The first pass was always on the steel side and the second pass was on the nickel alloy side. In each pass of the welding procedure a specific threaded polycrystalline cubic boron nitride (pcBN) tool (Q70), containing 30% Re as bind material [3] and probe lengths of 3 and 4 mm to weld the nickel and steel sides, respectively, were used. The welding process parameters on the Inconel 625 and API X65 steel sides were as follows: Rotational Speed [rpm]: 200 and 400; Welding Speed [mm/s]: 2 and 8; Force [kN]: 60 and 40; angle [°]: 0.5 both. As shielding gas, argon was applied.

2.3. Microstructural characterization

The cross-sectioned samples were etched with Nital 2% and Adler solutions to reveal the microstructure of the steel and the nickel alloy, respectively. Due it to the high aggressively of the etching solution used on the Inconel 625, an etching procedure was created to avoid over etching the steel. First, the steel side was covered with tape and the Inconel 625 was etched, after that, the tape was removed and the steel side was cleaned with ethanol for later being etched with Nital 2%. A light optical microscopy (OM) Keyence VHX-6000 and a scanning electron microscope (SEM) Quant 650 FEG, equipped with energy

dispersive spectroscopy (EDX), were used to analyze the base metal (BM) and the welded samples. Besides that, semi quantitative analyses of the main elements were.

2.4. Microhardness map

The microhardness maps were carried out on the cross-section of the weld using $HV_{0.5}$ with load of 500 gf and 0.5 mm indentation distance with the Struers DuraScan 70 machine.

3. Results and discussions

3.1. Friction welding process

The previously mentioned process parameters lead to a stable welding process to join the cladded plates. The calculated heat input is based on the process parameters and machine torque during welding [21]: 0.72 kJ/mm for the steel side, 1.19 kJ/mm for the Inconel 625 side. Previous studies showed that low heat input values (below 2.30 kJ/mm) are important to guarantee sound joints which are free of porosity, in particular in the Inconel 625 welds [22]. As shown in Figure 1, the welds present a good visual quality without external defects. According to the ISO 25239-3, 50 mm from the beginning and 50 mm from the end of the weld were removed and not considered further for testing and analysis.

Fig. 1 (a) 1st FSW pass on API X65 steel side. (b) 2nd FSW pass on Inconel 625.

3.2. Macrostructure and Microstructure observations

The resulting microstructures are related to the severe plastic deformation, material flow and thermal cycle imposed during the welding process. Fig. 2(a) shows a cross-sectional macrograph of the weld. At the top the 1st and 2nd deposition layers of Inconel 625 and at the bottom side the API 5L X65 substrate can be observed. Besides that, the typical appearance of the stir zone within the 1st (SZi-1st L) and 2nd (SZi-2nd L) Inconel 625 layer as well as within the base material of the 1st and 2nd Layer Inconel (BMi) are shown in Fig. 2 (b-e).

For the API 5L X65 steel side, also the stir zone (SZs), thermo-mechanically affected zone ($TMAZ_2$), heat affected zone (HAZ) and the base material of steel (BMs) are marked in the macrograph, see Fig.2(a).
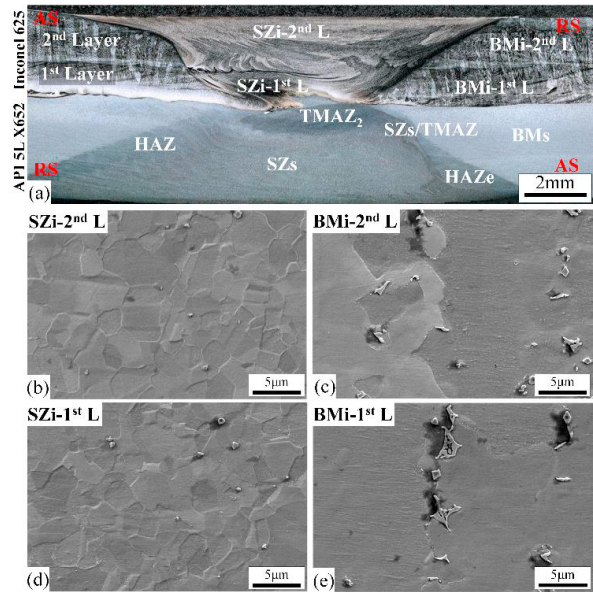

Fig. 2 (a) Macrograph of the weld, showing the Inconel 625 layers and the different Inconel welding zones at the top and the API 5L X65 at the bottom of the weld. The SEM micrographs (b-e) show the Inconel zones in detail. 2nd layer stir zone of the Inconel 625 (SZi-2nd L); 1st layer stir zone of the Inconel 625 (SZi-1st L); 2nd layer Inconel base material (BMi-2nd L); 1st layer Inconel base material (BMi-1st L); stir zone of the steel (SZs); second thermo-mechanically affected zone ($TMAZ_2$), heat-affected Zone (HAZ), external heat-affected Zone (HAZe) and base material of steel (BMs). Retreating side (RS); advancing Side (AS).

The detailed SEM microstructure images of the Inconel 625 stir zones are presented in Fig. 2 (b-d), while Fig. 2 (e) presents the Inconel 625 base material. The BMi layers present a columnar dendritic microstructure resulted from the Inconel 625 GTAW coating solidification. In the first layer, close to the API 5L X65 substrate, smaller dendrites are presented since the nucleation rate was higher than the growth rate, but this behavior changes further away from the fusion line and less, but bigger, dendrites can be observed due the fact that the nucleation rate was lower than the growth rate [23]. An average hardness of 250 $HV_{0.5}$ was measured in the Inconel 625 CRA layer.

Fig.2 (c) and (e) show the presence of secondary phases and precipitates in the BMi layers, which are accumulated in the interdendritic region of the Ni matrix. The 1st layer formed more and bigger secondary phases than the 2nd layer. This behavior might be related with the higher dilution of the steel elements inside the first CRA layer and with the heat input by GTAW deposition of the second clad layer. During the solidification of Inconel 625, elements such as Nb and Mo are segregated into the interdendritic region and this enrichment of elements concentration increases the number of secondary phases [24]. The EDX chemical analysis, presented in Fig. 3, indicates that a higher amount of Fe is diluted in the 1st layer of Inconel 625, 18.9 wt-% compared to 6.83 wt-% in the 2nd layer.
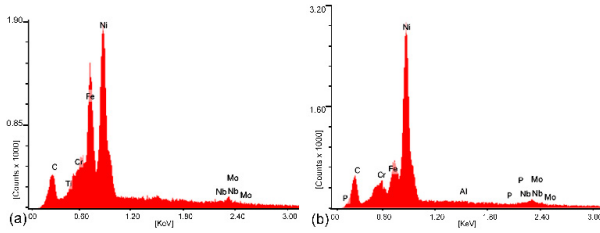
Fig. 3 EDX chemical analysis results of (a) 1st and (b) 2nd layer of deposited Inconel 625.

Most of the secondary phases and precipitates found are Laves and Nb-rich MC carbides. According to [1, 2], MC carbides and Laves are common in Fe-Ni alloys. Laves normally appear during solidification or during high temperatures exposition. This phase is typically characterized by large intergranular particles as seen in the Fig. 2 (c) and (e).

The Fig. 2 (b) presents the SZi-2nd L and (d) the SZi-1st L that both are representative image of the stir zone microstructure. The microstructures of the stir zone of the Inconel 625 weld (SZi-2nd L: Fig. 2 (b) and SZi-1st L: Fig. 2 (d)) show the change of the dendritic microstructure in the base material to refined equiaxed grains including some twinning grains. This change is mainly attributed to dynamic recrystallization imposed by the process [18]. This leads overall to a size reduction of the grains. The microstructure close to the steel substrate, SZi-1st L, exhibit more secondary phases and precipitates than the SZi-2nd L. The precipitates are mostly localized at the grain boundaries, but also small round precipitates are distributed inside some grains. This shows that the FSW process promotes the break and distribution of precipitates, which leads to an improvement of the mechanical properties of the material [25].

The base material API 5L X65, BMs, consists mainly of ferrite and some perlite, as shown in Fig. 4(a). The etching also revealed a second thermo-mechanically affected zone (TMAZ₂), Fig.4 (b), inside the steel weld and nearest to the interface between the CRA and the steel. It is believed that this TMAZ₂ occurred due to the 2nd welding pass. This TMAZ₂ appears with a darker color and shows a geometry similar to the tool tip. The microstructure in this region is classified as being ferrite and perlite like the BM, but with some reduction in grain size as can be seen in Fig. 4 (b).

The TMAZ formation in the API 5L X65 steel in this study shows a formation of mainly bainite (B) and some Widmanstätten ferrite (W). Additionally some acicular ferrite is observed, which some authors [26, 27] prefer to call idiomorphic primary ferrite (PF(I)) since in this process the reactions were completed at purely reconstructive transformation temperatures. The same microstructures are observed in the SZs, Fig.4 (e), and the HAZe, Fig.4(f). But, in the HAZe a greater amount of bainite with minor size is additional detected. In Fig.4 (d) a section that is exactly between the SZs and TMAZ is noted that shows a reduction in the grains size when compared with other mentioned zones.
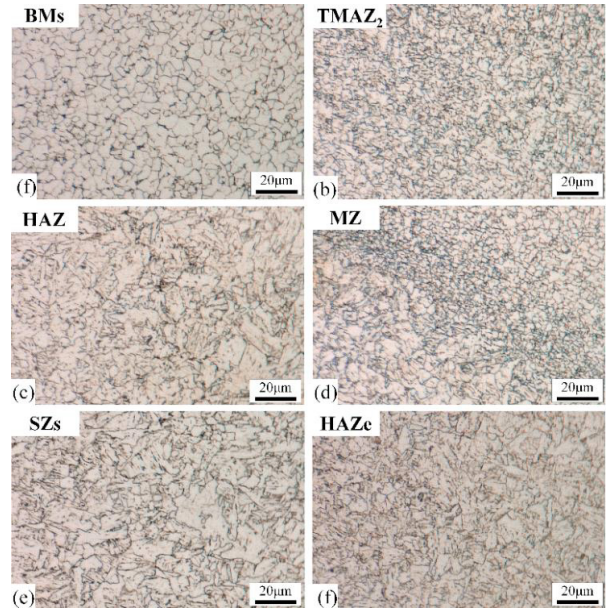

Fig. 4 Different microstructure from API 5L X65 steel. (a) Base material from steel (BMs), (b) Second thermo-mechanically affected zone (TMAZ₂), (c) heat-affected zone (HAZ), (d) section between the SZs and TMAZ, (e) stir zone of the steel (SZs) and (f) external heat-affected Zone (HAZe).

3.3. Microhardness tests

In Figure 5 the hardness distribution along the cross-section of the weld is depicted. The full thickness of the plate, with the Inconel 625 nickel alloy at the top and the API 5L X65 at the bottom is displayed. The minimum hardness of 160 $HV_{0.5}$ is observed in steel, where the maximum hardness of 382 $HV_{0.5}$ is present in Inconel. The average base material hardness increased in the stir zone and in the heat-affected zone of both materials due to grains size reduction and further microstructural transformations [3, 18].
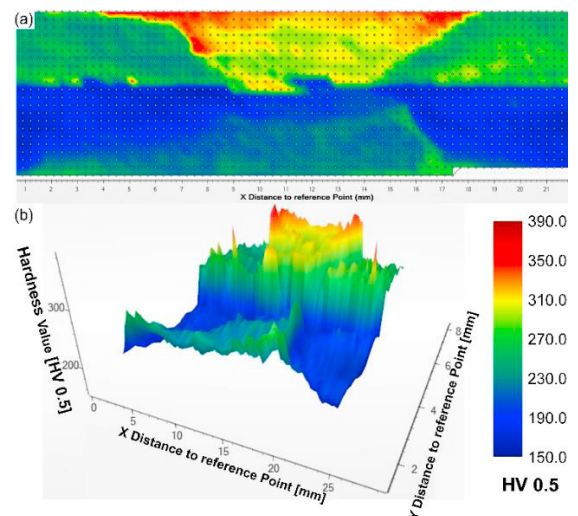

Fig. 5 Microhardness map of FSW API 5L X65/Inconel 625.

The microhardness test corroborates with the microstructural results obtained in Figure 4. The HAZe in API 5L X65 steel shows the highest microhardness value, approximately 270 HV.

In Inconel X65 the highest microhardness value is 382 HV in the Inconel heat-affected zone (HAZi) while in the SZi-2nd L the hardness is only 290 HV, see Fig. 6 (b) and (c), attributed to the grain size and the phases transformation in the steel.
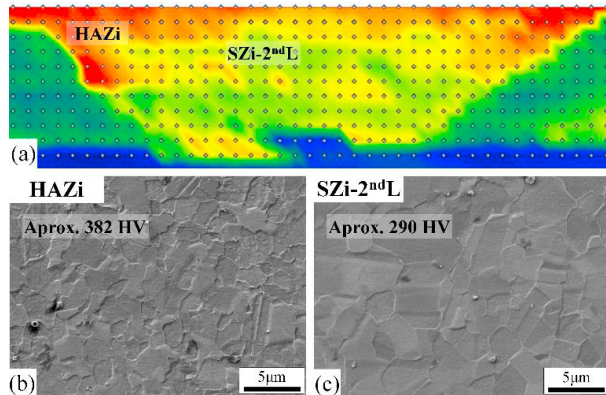

Fig. 6 (a) Microhardness map of Inconel 625. (b) HAZi and (c) SZi-2nd L.

4. Conclusions

The present work investigates the effectiveness of a two-pass Friction Stir Welding process, applied for the first time to API 5L X65 steel plates cladded with Inconel 625. Microstructural characterization and mechanical tests were conducted and showed an improvement of the mechanical properties in the weld region compared to the base materials. The following key observations are made:

- Limited material mixing and inter-diffusion have been observed at the interface between Inconel 625 and API 5L X65 steel, as a result of the two-pass FSW procedure.
- The welding process changed the microstructure of the Inconel and the API X65 steel, where a recrystallized refined grains region was achieved in the stir zone. A complex microstructure composed by ferrite (F), bainite (B), Widmanstätten ferrite (W) and idiomorphic primary ferrite PF(I) was observed within the steel weld. The FSW process imposed transformation from a dendritic to an equiaxial microstructure in the Inconel 625 weld.
- The hardness of the materials increased inside both welding zones.
- FSW caused drastic changes in microstructure, increase in microhardness, grains size reduction, break and homogeneous distribution of precipitates. All of these changes tend to improve the mechanical properties.

Acknowledgements

References

[1] DuPont JN, Lippold JC, Kiser SD. Welding Metallurgy and Weldability of Nickel-Base Alloys. New Jersey: John Wiley & Sons, 2009.

[2] Song KH, Nakata K. Effect of precipitation on post-heat-treated Inconel 625 alloy after friction stir welding. Mater Des 2010; 31: 2942–2947.

[3] Lemos GVB, Hanke S, Dos Santos JF, et al. Progress in friction stir welding of Ni alloys. Sci Technol Weld Join 2017; 22: 643–657.

[4] DNV-OS-F101. DNV-OS-F101: Submarine pipeline systems. Det Nor Verit 2013; 367.

[5] Guo L, Zheng H, Liu S, et al. Effect of heat treatment temperatures on microstructure and corrosion properties of inconel 625 weld overlay deposited by PTIG. Int J Electrochem Sci 2016; 11: 5507–5519.

[6] API 5L - American Petroleum Institute. Specification for Line Pipe. 2000.

[7] Dupont JN. Solidification of an alloy 625 Weld Overlay. Metall Mater Trans A Phys Metall Mater Sci 1996; 27: 3612–3620.

[8] Petrzak P, Kowalski K, Blicharski M. Analysis of phase transformations in Inconel 625 alloy during annealing. Acta Phys Pol A 2016; 130: 1041–1044.

[9] Cieslak MJ, Ritter AM, Savage WF. Solidification Cracking and Analytical Electron Microscopy of Austenitic Stainless Steel Weld Metals. Weld J (Miami, Fla); 61.

[10] Maltin CA, Galloway AM, Mweemba M. Microstructural evolution of inconel 625 and inconel 686CPT weld metal for clad carbon steel linepipe joints: A comparator study: The effect of iron dilution on the elemental segregation of alloying elements in nickel based filler metals. Metall Mater Trans A Phys Metall Mater Sci 2014; 45: 3519–3532.

[11] Dutra JC, Silva RHG e., Marques C, et al. A new approach for MIG/MAG cladding with Inconel 625. Weld World 2016; 60: 1201–1209.

[12] Mortezaie A, Shamanian M. An assessment of microstructure, mechanical properties and corrosion resistance of dissimilar welds between Inconel 718 and 310S austenitic stainless steel. Int J Press Vessel Pip 2014; 116: 37–46.

[13] Anbarasan N, Jerome S, Arivazhagan N. Argon and argon-hydrogen shielding gas effects on the laves phase formation and corrosion behavior of Inconel 718 gas tungsten arc welds. J Mater Process Technol 2019; 263: 374–384.

[14] Mills WJ. Effect of Heat Treatment on the Tensile and Fracture Toughness Behavior of Alloy 718 Weldments. Weld J 1984; 63.

[15] Silva CC, Afonso CRM, Ramirez AJ, et al. Assessment of microstructure of alloy Inconel 686 dissimilar weld claddings. J Alloys Compd 2016; 684: 628–642.

[16] Liu FC, Hovanski Y, Miles MP, et al. A review of friction stir welding of steels: Tool, material flow, microstructure, and properties. J Mater Sci Technol 2018; 34: 39–57.

[17] Song KH, Nakata K. Mechanical Properties of Friction-Stir-Welded Inconel 625 Alloy. Mater Trans 2009; 50: 2498–2501.

[18] Rodriguez J, Ramirez AJ. Microstructural characterisation of friction stir welding joints of mild steel to Ni-based alloy 625. Mater Charact 2015; 110: 126–135.

[19] Sato YS, Arkom P, Kokawa H, et al. Effect of microstructure on properties of friction stir welded Inconel Alloy 600. Mater Sci Eng A 2008; 477: 250–

258.

[20] Hanke S, Lemos GVB, Bergmann L, et al. Degradation mechanisms of pcBN tool material during Friction Stir Welding of Ni-base alloy 625. Wear 2017; 376–377: 403–408.

[21] Cunha PHCP Da, Lemos GVB, Bergmann L, et al. Effect of welding speed on friction stir welds of GL E36 shipbuilding steel. J Mater Res Technol 2019; 8: 1041–1051.

[22] Lemos GVB, Farina AB, Martinazzi D, et al. Efeito da Velocidade de Rotação da Ferramenta na Soldagem por Fricção e Mistura Mecânica da Liga Inconel 625. In: ABM (ed) 71º Congresso Anual da ABM – Internacional. Rio de Janeiro, 2016, pp. 1387–1395.

[23] Kim JS, Lee HW. Effect of Welding Heat Input on Microstructure and Texture of Inconel 625 Weld Overlay Studied Using the Electron Backscatter Diffraction Method. Metall Mater Trans A Phys Metall Mater Sci 2016; 47: 6109–6120.

[24] Silva CC, de Albuquerque VHC, Miná EM, et al. Mechanical Properties and Microstructural Characterization of Aged Nickel-based Alloy 625 Weld Metal. Metall Mater Trans A Phys Metall Mater Sci 2018; 49: 1653–1673.

[25] Sundararaman M, Mukhopadhyay P, Banerjee S. Carbide Precipitation in Nickel Base Superalloys 718 and 625 and Their Effect on Mechanical Properties. Miner Met Mater Soc 1997; 367–378.

[26] Thewlis G. Materials perspective: Classification and quantification of microstructures in steels. Mater Sci Technol 2004; 20: 143–160.

[27] Bhadeshia H, Honeycombe R. Steels: Structure and Properties. 4th ed. Elsevier Ltd. Epub ahead of print 2017.